

# Parallel pathways convey olfactory information with opposite polarities in *Drosophila*

Kaiyu Wang<sup>a,b</sup>, Jiaxin Gong<sup>a,b</sup>, Qingxiu Wang<sup>a</sup>, Hao Li<sup>a,b</sup>, Qi Cheng<sup>a,b</sup>, Yafeng Liu<sup>c,d</sup>, Shaoqun Zeng<sup>c,d</sup>, and Zuoren Wang<sup>a,1</sup>

<sup>a</sup>Institute of Neuroscience and State Key Laboratory of Neuroscience, Shanghai Institutes for Biological Sciences, Shanghai 200031, China; <sup>b</sup>University of Chinese Academy of Sciences, Shanghai 200031, China; <sup>c</sup>Britton Chance Center for Biomedical Photonics and <sup>d</sup>Department of Biomedical Engineering, Huazhong University of Science and Technology-Wuhan National Laboratory for Optoelectronics, Wuhan 430074, China

Edited by John G. Hildebrand, University of Arizona, Tucson, AZ, and approved January 8, 2014 (received for review October 2, 2013)

**In insects, olfactory information received by peripheral olfactory receptor neurons (ORNs) is conveyed from the antennal lobes (ALs) to higher brain regions by olfactory projection neurons (PNs). Despite the knowledge that multiple types of PNs exist, little is known about how these different neuronal pathways work cooperatively. Here we studied the *Drosophila* GABAergic mediolateral antennocerebral tract PNs (mlPNs), which link ipsilateral AL and lateral horn (LH), in comparison with the cholinergic medial tract PNs (mPNs). We examined the connectivity of mlPNs in ALs and found that most mlPNs received inputs from both ORNs and mPNs and participated in AL network function by forming gap junctions with other AL neurons. Meanwhile, mlPNs might innervate LH neurons downstream of mPNs, exerting a feedforward inhibition. Using dual-color calcium imaging, which enables a simultaneous monitoring of neural activities in two groups of PNs, we found that mlPNs exhibited robust odor responses overlapping with, but broader than, those of mPNs. Moreover, preferential down-regulation of GABA in most mlPNs caused abnormal courtship and aggressive behaviors in male flies. These findings demonstrate that in *Drosophila*, olfactory information in opposite polarities are carried coordinately by two parallel and interacted pathways, which could be essential for appropriate behaviors.**

circuit | electrical coupling | electrophysiology | multicolor calcium imaging | multiglomerular

In insects, the detection of olfactory cues begins at the peripheral olfactory receptor neurons (ORNs), which transfer the chemical information into neural signals and convey them to the first central relay station—the antennal lobes (ALs) (1–3). After AL local processing, olfactory information is relayed to higher brain regions via different groups of projection neurons (PNs) (4–6). Except some pioneering studies in Hymenoptera (7–11) and Lepidoptera (12), little is known about how these different PNs connect in the olfactory circuit and work physiologically. As the most studied PN type in *Drosophila*, the cholinergic PNs (mPNs) form the medial antennocerebral tract and convey excitatory signals encoding odor identity and intensity (13–15) that are necessary for the fly to perform appropriate behaviors (16, 17). However, how olfactory information is delivered via pathways mediated by PNs other than mPNs remains to be elucidated. In this study, we focused on the mediolateral antennocerebral tract PNs (mlPNs), which are the second largest PN subset (~50 mlPNs in each hemisphere) and reported to be largely GABAergic with axons terminating mainly in the lateral horn (LH) (18, 19). Based on the extent of their dendritic arborization, mlPNs can be further categorized into three subtypes: the uniglomerular mlPNs (type 1 mlPNs, mlPN1s); the multiglomerular mlPNs (mlPN2s), which comprise the great majority (>80%) of mlPNs; and the panglomerular mlPNs (mlPN3s) (19). Here we focused on mlPN1s and mlPN2s, which exclusively link ALs with the ipsilateral LH and were labeled by *Mz699-Gal4* (hereafter referred to as Mz699-mlPNs, or mlPNs) (20). Using dual whole-cell recordings and optogenetic activation of mlPNs, we examined their connectivity

with different groups of AL and LH neurons and identified their main excitatory input neurons and putative output targets. The odor responses of mlPNs were also characterized and compared with those of ORNs and mPNs by dual-color imaging. Finally, we investigated the physiological role of mlPNs at the behavioral level by preferentially silencing the inhibitory output of mlPNs. Our results showed that by conveying olfactory information as inhibitory signals in parallel with the excitatory mPN pathway, the mlPN pathway might play important roles in modulating fly behavior through a novel feedforward inhibition mechanism.

## Results

**mlPNs Receive Multiple Excitatory Inputs.** Anatomical studies have shown that mlPNs send dendrites into single or multiple glomeruli of the ipsilateral AL (19), where they probably receive inputs from ORNs and other AL neurons. We first examined whether, like mPNs (21), mlPN dendrites receive direct ORN inputs. Dual whole-cell recordings were made on an Mz699-mlPN and an mPN located anterior-dorsal to the AL (Fig. 1A). We then applied brief pulse stimulations (50  $\mu$ s) to the ipsilateral antennal nerve with a suction electrode to excite all ORN axons from the antenna (21) (Fig. 1A). Electrical stimulation elicited inward currents in both the mlPN and the mPN with short latency (<3 ms; Fig. 1B), suggesting monosynaptic ORN–mlPN connections. In all eight pair recordings, we found responses in both PNs, although the delay of onset of inward currents in some mlPNs was longer (>4 ms), probably reflecting polysynaptic responses (Fig. 1C).

Because the dendrites of mPNs also serve as presynaptic elements within ALs (22), we asked whether mlPNs receive lateral inputs from mPNs. To activate mPNs while performing whole-

## Significance

Olfactory information is relayed from the antennal lobes (ALs) to higher regions via parallel pathways formed by different projection neurons (PNs) in insects. Here we have systematically investigated the functional connectivity, odor responses, and behavioral significance of GABAergic mediolateral PNs that link AL with the lateral horn in *Drosophila*. Our findings demonstrated that the two pathways formed by GABAergic PNs and cholinergic PNs, respectively, shared the same primary input, interacted with each other via cholinergic and electrical synapses, and carried olfactory information coordinately in opposite polarities. This organization could be important for olfactory processing and proper behavior.

Author contributions: K.W. and Z.W. designed research; K.W., J.G., Q.W., H.L., and Q.C. performed research; Y.L. and S.Z. contributed new reagents/analytic tools; K.W., J.G., and H.L. analyzed data; and K.W. and Z.W. wrote the paper.

The authors declare no conflict of interest.

This article is a PNAS Direct Submission.

<sup>1</sup>To whom correspondence should be addressed. E-mail: zuorenwang@ion.ac.cn.

This article contains supporting information online at [www.pnas.org/lookup/suppl/doi:10.1073/pnas.1317911111/-DCSupplemental](http://www.pnas.org/lookup/suppl/doi:10.1073/pnas.1317911111/-DCSupplemental).

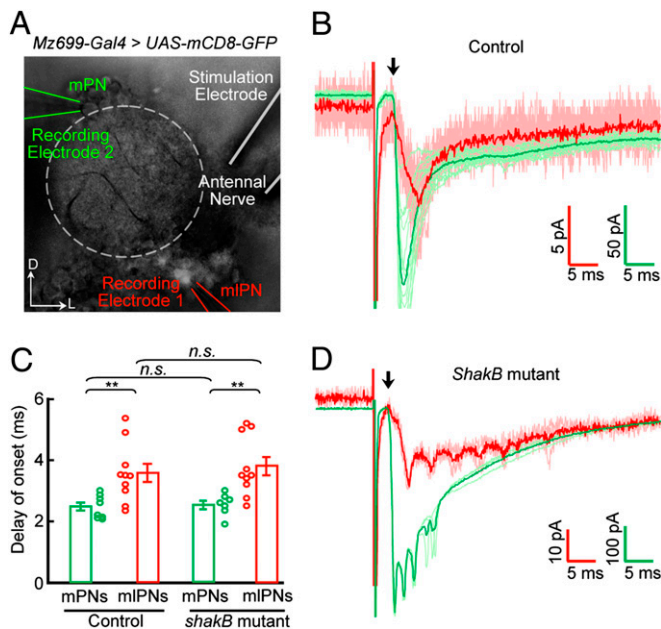


**Fig. 1.** Monosynaptic connection from ORNs to Mz699-mIPNs. (A) Dual whole-cell recordings were performed on an Mz699-labeled mIPN (indicated with the red electrode) and an mPN (green electrode), while the ipsilateral antennal nerve was stimulated (white electrode). The antennal lobe is outlined with dashed lines. (B) Sample traces showing stimulation-evoked inward currents in an mIPN (red) and mPN (green) in a control brain. Darker traces are averaged from lighter ones of the same color. Arrow indicates the start of the inward current. (C) Bar plot showing averaged delay of onset of inward currents of mPNs and mIPNs (open circles) of the indicated genotypes (mean  $\pm$  SEM). Asterisks indicate significant differences (\*\* $P < 0.01$ ; n.s., not significant). (D) Similar to B except that the traces were obtained from a *shakB*<sup>2</sup>-deficient brain, which lacks mPN–mIPN gap junctions.

cell recording of Mz699-mIPNs, we expressed ChIEF—an improved version of channelrhodopsin with a large plateau conductance and a fast closing rate (23)—in defined mPNs and used laser stimulation ( $\sim 473$  nm) precisely controlled by an acousto-optic deflector (AOD) system to activate them (24). Laser illumination induced depolarization and spiking in ChIEF-expressing mPNs, but not in mPNs from brains without ChIEF expression (Fig. S1 A and B). By using this experimental system, we found that firing of a large group of *GH146-QF*-labeled mPNs (25) evoked marked depolarization in most recorded Mz699-mIPNs; the depolarization was significantly reduced after blocking cholinergic neurotransmission with the antagonist mecaminylamine (50  $\mu$ M; Fig. 2A). However, we noticed a quick residual response (delay  $< 1$  ms) in most recorded Mz699-mIPNs even in the presence of the antagonist, suggesting mPN–mIPN gap junctions. To test this, we loaded a small-molecule tracer (biocytin or neurobiotin) (15) into single mPNs during whole-cell recording and examined its diffusion into Mz699-mIPNs labeled with GFP. The tracer was found in Mz699-mIPNs in 23 of 29 examined control brains (Fig. 2B and D), but not in the *shakB*<sup>2</sup> brains (26) with no functional gap junctions between mPNs and mIPNs (Figs. 2C and D and 3A). Therefore, some Mz699-mIPNs receive both cholinergic and electrical inputs from mPNs.

The electrical coupling of Mz699-mIPNs to mPNs provides another possible explanation for the short delay ( $< 4$  ms) of the inward current observed in these mIPNs (Fig. 1D): mPNs, rather than mIPNs, receive direct inputs from ORNs and then spread the current to mIPNs through electric coupling. We repeated the antennal-nerve stimulation experiment in *shakB*<sup>2</sup> mutant brains and found that the distribution of the delay of onset was not significantly different between mutant flies and controls (Fig.

1D). Many recorded Mz699-mIPNs still exhibited short delays ( $< 3$  ms), indicating they receive monosynaptic ORN inputs, whereas several Mz699-mIPNs had longer delays ( $> 4$  ms) (Fig. 1C and D), suggesting excitatory inputs from palp ORNs or other AL neurons, such as mPNs (22, 27). Thus, mIPNs receive multiple excitatory inputs, including direct ORN inputs and lateral inputs from other AL neurons.

**Dendrites of mIPNs Form a Selective Electrical Network.** Because some Mz699-mIPNs are electrically coupled to mPNs, and a single mIPN2 innervates multiple glomeruli (19), these mIPNs might form a local electrically coupled network allowing neuronal activity to propagate among selective glomeruli. If this is the case, two characteristics would be expected: First, the electrical coupling between mIPN2s and mPNs is reciprocal; second, a single mIPN2 forms electrical synapses with multiple mPNs that innervate different glomeruli (heterotypic mPNs). To examine these characteristics, we used optogenetic tools to manipulate the activity of mIPNs and simultaneously measured the responses in mPNs with whole-cell recordings (Fig. 3A). In the brains with ChIEF expression in Mz699-mIPNs (*Mz699-Gal4 > ChIEF-tdTomato*), restrictive blue laser illumination of the AL, where the dendrites of ChIEF-positive mIPNs are located, resulted in spiking of these mIPNs (Fig. S1C) and depolarization of some mPNs with short delay of onset ( $< 1$  ms) in a mecaminylamine-insensitive manner (Fig. 3A). In contrast, restrictive illumination

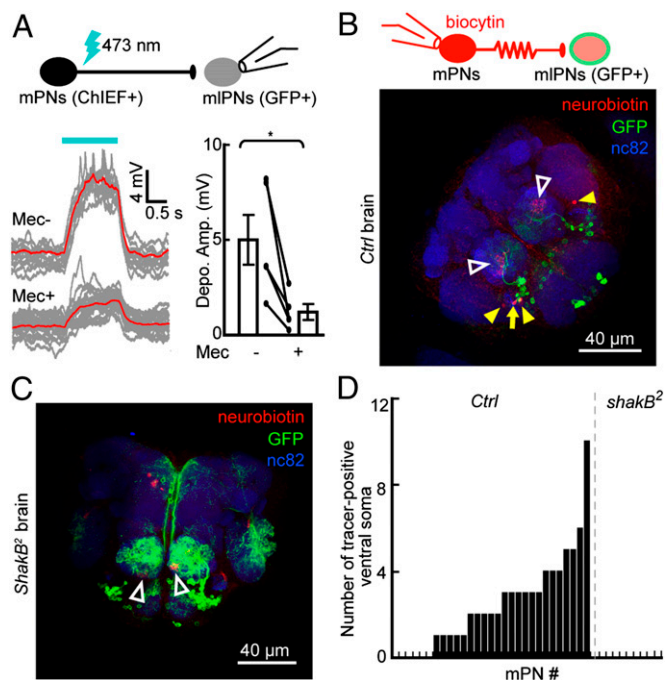


**Fig. 2.** Dendrites of Mz699-mIPNs receive cholinergic and electrical inputs from mPNs. (A) Whole-cell recordings were performed on an Mz699-mIPN, while ChIEF-positive mPNs in a *GH146-QF > ChIEF-tdTomato* brain were stimulated with a laser (Upper). Depolarizations and spiking were observed in recorded mIPNs. Sample traces (Left, red trace is averaged from gray traces) and plots (Right) show that the depolarization amplitude (Depo. Amp.) was reduced but not eliminated after application of the cholinergic blocker mecaminylamine (Mec;  $n = 5$ ; mean  $\pm$  SEM; \* $P < 0.05$ ). (B) Illustration (Upper) and fluorescence image (Lower) show that the tracer loaded into a single mPN by whole-cell recording was detected in an Mz699-mIPN soma (arrow) and other somata (solid arrowheads). Open arrowheads indicate the glomeruli of recorded mPNs. (C) Similar to B except that the recordings were performed on a *shakB*<sup>2</sup>-deficient brain. (D) Bar plots summarizing the number of tracer-positive mIPNs after loading of a single mPN for  $\sim 1$  h, in both control and *shakB*<sup>2</sup> mutant brains.

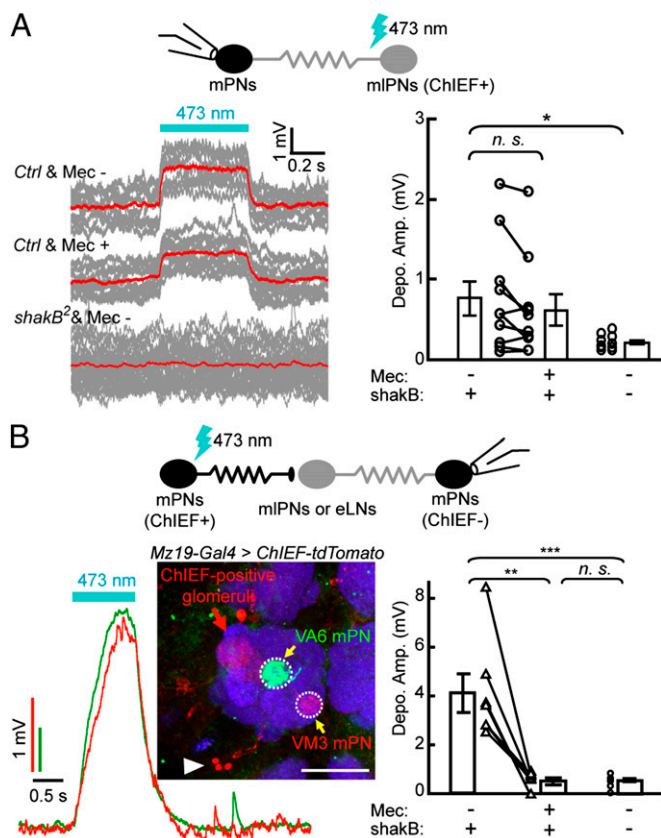


**Fig. 3.** Activity of Mz699-mIPNs influence mPNs via gap junctions. (A) Whole-cell recordings were performed on an mPN, while ChIEF-positive mIPNs in an *Mz699-Gal4 > ChIEF-tdTomato* brain were activated by laser stimulation (Upper). Mecamylamine (Mec)-insensitive depolarizations were observed in mPNs in control brains but not in *shakB*<sup>2</sup> mutant brains, as shown by sample traces (Left) and plots (Right) ( $n = 10$  per group). (B) Laser illumination of ChIEF-positive mIPNs innervating defined glomeruli (DA1, VA1d, and DC3 glomeruli, as indicated by the red arrow) depolarized other heterotypic mPNs (in the VM3 and VA6 glomeruli, indicated by yellow arrows). Sample traces (Left) were obtained simultaneously from VM3 (red) and VA6 (green) mPNs. White arrowhead indicates somata of dye-coupled neurons. Plots (Right) summarizing peak depolarization amplitudes in mPNs caused by laser stimulation of other heterotypic mPNs in control and *shakB*<sup>2</sup> mutant brains, in the absence or presence of a cholinergic antagonist (Mec;  $n = 6$ ). Horizontal blue bars above traces indicate laser illumination. (Scale bars, 20  $\mu$ m.) Data in plots are shown as mean  $\pm$  SEM; \* $P < 0.05$ ; \*\* $P < 0.01$ ; \*\*\* $P < 0.001$ ; n.s., not significant.

of the somata of the recorded mPNs induced much smaller depolarizations than those caused by AL illumination (Fig. S1D). To further exclude the possibility that the mPN depolarizations were caused by activation of ChIEF proteins in these mPNs due to leak expression, we repeated the experiment in *shakB*<sup>2</sup> mutant brains and found no obvious depolarization in mPNs (Fig. 3A). Because mIPNs are GABAergic and lack dendritic presynaptic sites in the AL (28), the mPN depolarization could only be caused by mIPN–mPN coupling via gap junctions. We showed above (Fig. 2A) that the mPN activity can spread to mIPNs through gap junctions, thus the electrical coupling between mIPNs and mPNs is reciprocal.

We next examined whether the activity in single mIPN2 can spread to heterotypic mPNs via gap junctions. The *Np1580-Gal4* line (19), which exclusively labels a group of mIPN2s innervating a defined set of glomeruli (Fig. S1E), was used to drive ChIEF-tdTomato expression. Activation of these mIPN2s induced marked depolarizations in mPNs that innervated any one of the ChIEF-positive glomeruli (Fig. S1E), as well as small depolarizations in

mPNs that did not innervate ChIEF-positive glomeruli (Fig. S1E). Excitatory local neurons (eLNs) form a global network with most if not all mPNs and may mediate crosstalk among glomeruli (29–31), but the small number of eLNs and the low efficacy of mPN–eLN coupling are insufficient for mediating crosstalk on a large scale (27, 32). If mIPNs indeed form a local electrically coupled network with mPNs, the crosstalk among heterotypic mPNs should be larger in amplitude and more selective. We found that, when  $\sim 13$  mIPNs innervating the three glomeruli labeled in *Mz19-Gal4* (the DA1, VA1d, and DC3 glomeruli) were optogenetically activated, heterotypic mIPNs innervating other ChIEF-negative glomeruli were depolarized in a selective manner (Fig. 3B and Fig. S2). This mIPN–mPN crosstalk was diminished when cholinergic neurotransmission was blocked or when functional gap junctions among mIPNs and mPNs were absent (Fig. 3B), suggesting the necessities of unidirectional mIPN–mIPN cholinergic neurotransmission and reciprocal mIPN–mPN electrical coupling in this crosstalk. Thus, by making bidirectional electrical connections with heterotypic mPNs, mIPN2s can form a selective electrical network linking multiple glomeruli within the AL. Also, the electrical activity of single mIPNs can spread to glomeruli other than the ones they innervate, probably via gap junctions among different mIPNs in addition to mIPN–mIPN gap junctions.

**Activity Is Effectively Transformed from ORNs to mIPNs.** To study the transfer of olfactory information from ORNs to mIPNs directly and quantitatively, we monitored the odor-evoked activity patterns in ORN axons and mIPN dendrites simultaneously by dual-color calcium imaging (33). We used two independent binary expression systems (LexA/LexAop and Gal4/UAS) (18) to express G-CaMP3 and R-GECO1, two calcium indicators that have different excitation/emission spectra but similar response dynamics (34–36) (Fig. S3A and B) in *Orco-LexA* labeled ORNs and Mz699-mIPNs, respectively (Fig. S3C). Seventeen different odors were presented to each fly, and the response patterns of ORNs and mIPNs were measured. The odor-evoked responses of mIPNs as shown by R-GECO1 signals were robust and odor selective (Fig. S3D). Moreover, the activity patterns in mIPN dendrites were generally similar to those in ORN axons (Fig. S3D), suggesting an effective activity transfer from ORNs to mIPNs. Further quantitative analysis showed that the response profiles in mIPNs were relatively broader than those in ORNs (Fig. S3E and F), indicating that mIPNs have relatively lower odor selectivity than ORNs. These findings are consistent with the more global dendritic arborization of mIPN2s than of ORNs (18, 19).

#### Olfactory Information Is Conveyed via Parallel mIPN and mPN Pathways.

To understand how olfactory information is conveyed to higher brain centers via mIPNs and mPNs, we first examined the odor-evoked activities of mIPN1s, which, like mPNs, are monoglomerular. By expressing R-GECO1 in a single mIPN innervating the VA1d glomerulus (*Np839-Gal4 > R-GECO1*) (19) and G-CaMP3 in a large fraction of mPNs in the VA1d glomerulus (*GHI46-LexA > G-CaMP3*), we visualized the activities of the mIPN and mPNs simultaneously (Fig. S4A). The mIPN dendrites in the VA1d glomerulus exhibited an odor-response profile comparable to that of the VA1d mPNs (Fig. S4B and C). Similar results were obtained by comparing the response profiles of the mIPN and mPNs innervating the VA1v glomerulus (Fig. S4D).

Next we examined odor-evoked responses in mIPN2s, which innervate multiple glomeruli. Because several Gal4 lines reported to selectively label mIPN2s (19) did not express enough calcium indicator for reliable imaging in our experiments, we used *Mz699-Gal4*, which labels several mIPN1s and  $\sim 30$  mIPN2s. By performing dual-color in vivo imaging that covered most of the ALs (Fig. S5A), we found that both mIPNs and mPNs exhibited robust and selective odor-evoked responses (Fig. S5B). Comparison of the odor-evoked responses of mIPNs and mPNs

in defined glomeruli that contained the dendrites of both showed that, in most cases, mIPNs exhibited broader odor tuning than mPNs did (Fig. 4A and Fig. S5C), suggesting that mIPN2s are less odor selective than mPNs and, by extension, mIPN1s. This finding was reproducible across different flies (Fig. 4B). The response intensity in both mIPNs and mPNs increased with elevating concentrations (Fig. 4C and D), indicating that these two types of PNs convey correlated inhibitory and excitatory information.

**Axons of mIPNs Target LH Neurons Downstream of mPNs.** To identify the targets of mIPN axons in LH, we first examined whether mIPN axons form synapses on mPN axons. By labeling mIPNs and mPNs with mCD8-GFP and tdTomato, respectively, we found that the putative presynaptic sites (varicosities) of mIPNs were largely separated from the mPN axons (Fig. 5). To assess mPN–mIPN interactions, we examined the distribution of mPN axon fluorescence surrounding mIPN varicosities and compared it with the

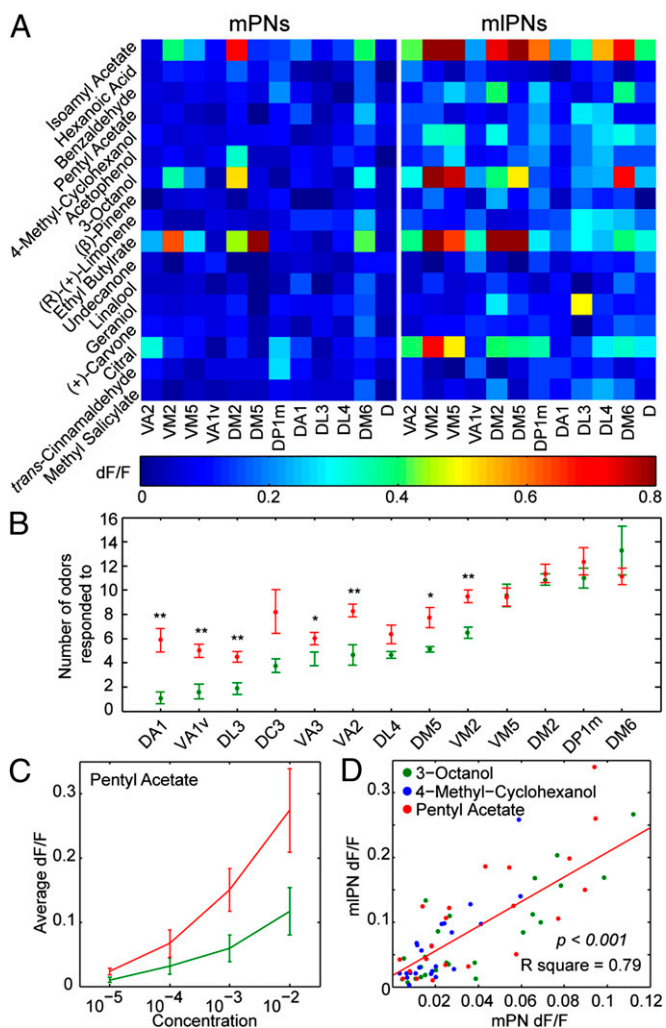


**Fig. 4.** Correlated odor-evoked activities in mIPN2s and mPNs. (A) Color maps summarizing the activities of mIPNs and mPNs in response to different odors in the indicated glomeruli (averaged from two ALs in one brain). (B) Plot shows the averaged number of odors that activated mIPNs (red) or mPNs (green) in defined glomeruli ( $n = 6$  ALs; mean  $\pm$  SEM;  $*P < 0.05$ ;  $**P < 0.01$ ). (C) The amplitude of the fluorescence response ( $dF/F_0$ ) in mIPNs (red) and mPNs (green) in a fraction of glomeruli are plotted against odor concentrations as indicated by dilution rate. (D) The change of response amplitudes to different odor concentrations in mIPNs is well correlated with the change in mPNs. The red line is a linear fit.

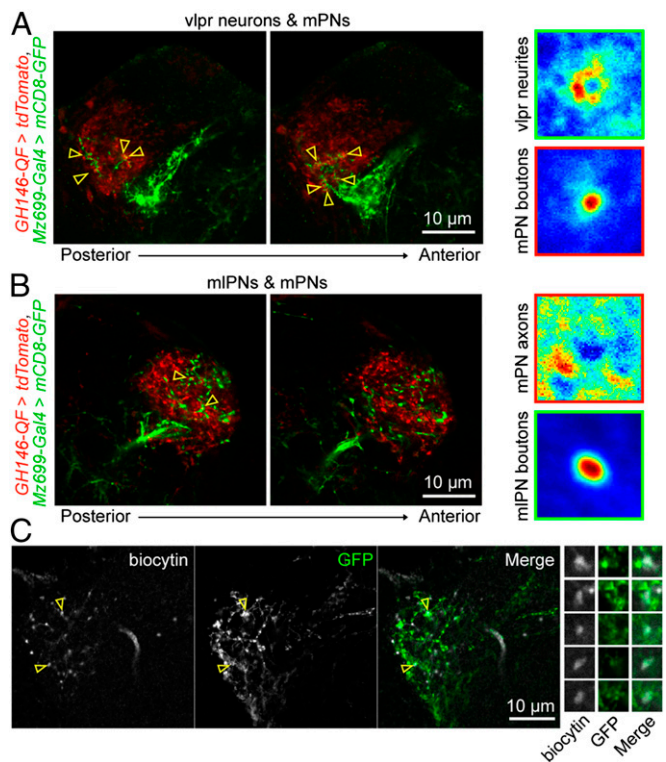


**Fig. 5.** Axons of mIPNs make appositions with LH neurons downstream of mPNs. (A, Left, posterior to anterior) Fluorescence images taken at different depths in the LH where mPN axons (red) and neurites of vIPr neurons (green) were labeled. (Right) Images (in false color) averaged from images centered on individual varicosities on mPN axons, showing that neurites of vIPr neurons closely surround varicosities on mPN axons. (B) Similar to A, except that mIPN axons rather than vIPr neurons are labeled (green). (C) Enlarged views showing potential contact sites between mIPN axons and neurites of a LH neuron downstream of mPNs, as well as fluorescence images of selected potential contact sites. Yellow open arrowheads indicate potential contact sites between the two populations of neurons.

fluorescence of mPN synaptic targets (neurons in ventrolateral protocerebrum, or vIPr neurons) surrounding mPN axon varicosities (37, 38). As expected, we found close appositions of vIPr neurons' neurite fluorescence around mPN varicosities (Fig. 5A), but no clear apposition of mPN axons around mIPN varicosities (Fig. 5B). Thus, mIPNs are unlikely to form synapses with mPN axons, but with other neurons innervating the LH.

We next asked whether mIPNs target neurons downstream of mPNs. To identify these downstream neurons, we performed whole-cell recordings on somata located around the LH and measured the responses evoked by optogenetic excitation of a large fraction of mPNs (Fig. S6A). Among 132 blindly recorded neurons from 55 brains, 46 showed detectable depolarizations in response to mPN firing, with variable delays of onset (Fig. S6B and C) that could be attributed to the latency of AP initiation in mPNs by laser stimulation or to polysynaptic excitation. We loaded tracer into the responsive neurons to visualize their neurites by post hoc staining. The majority (15/20) of those recorded neurons with relatively immediate responses after laser stimulation ( $<30$  ms) innervated LH (Fig. S6B). Further examination of the morphological interactions between the recorded LH neurons and the two types of PNs indicated that the axons of mPNs (ChIEF-tdTomato labeled) and mIPNs (GFP labeled) might target the same LH neurons (7 out of 15). An example is shown in Fig. 5C: one recorded neuron with neurite in the ipsilateral LH depolarized soon after mPNs fired (delay of onset = 12.5 ms), suggesting that it received direct or indirect excitatory

inputs from mPNs (Fig. S6A). Meanwhile, the putative contacts between its arborization and mPN axon terminals indicated that this LH neuron might also receive inputs from GABAergic mPNs. Thus, mPNs could target neurons downstream of mPNs and modulate their activity.

**Feedforward Inhibition from the mPN Pathway Modulates Male Behaviors.** Because LH is a region believed to mediate flies' olfactory-dependent innate behaviors (16, 39, 40), we reasoned that, if the mPN pathway plays important roles in olfactory processing, dysfunction of this pathway should cause behavioral abnormalities. We down-regulated GABA level in Mz699-mPNs with a small interfering RNA (siRNA) against glutamic acid decarboxylase (GAD) (41, 42), the GABA synthetase (Fig. S7A and B). Considering that behaviors such as courtship and fighting in male flies are more robust and obvious than those in females, we only examined the behavior of males here. Compared with control males, the *GAD-knockdown* (*GAD-KD*) males exhibited normal locomotion (Fig. S7C), elevated male–male courtship behavior, and enhanced aggressive behavior (Fig. S7D). The elevated courtship and aggressive behaviors in paired *GAD-KD* males could be caused by a disinhibition of these behaviors, a postulation supported by three additional lines of evidence. First, although as able as control males to distinguish sex, *GAD-KD* males spent more time interacting with target flies (both male and female) than control males did (Fig. S7D–G). Second, *GAD-KD* males exhibited courtship behaviors including unilateral wing extension, licking, and copulation attempts more frequently than control males (Fig. S7D). Third, even when orientated away from the target fly, *GAD-KD* males sometimes exhibited courtship behaviors including unilateral wing vibration, proboscis extension, and abdomen bending (Fig. S7D). Thus, the mPN pathway might be involved in controlling the level of male courting and fighting through feedforward inhibition. It should also be noted that the *Mz699-Gal4* line faintly labels several other GABAergic neurons besides mPNs (approximately two neurons innervating suboesophageal ganglion, approximately two neurons around LH, and approximately four neurons at the medial part of the mushroom body calyx) in the brain, and these other populations may also contribute to the inhibitory signaling in the *Drosophila* olfactory system, although we did not investigate them.

## Discussion

In many insects, olfactory information is transferred from ALs to higher regions via multiple PN pathways. For instance, by combining electrical/optical recordings and modeling, researchers found that in Hymenoptera, two separate pathways formed by uniglomerular PNs that innervating nonoverlapping glomeruli convey information with similar profiles, although the odor selectivity is higher in the medial pathway and the response delay is shorter in the lateral pathway (7–11). Also, recent progress in Lepidoptera suggest that two parallel olfactory pathways are responsible for the innate and learned behaviors, respectively (12). Here, by using genetic tools in *Drosophila*, we show that two defined subsets of PNs convey information cooperatively but with opposite polarities. First, most of both types of PNs receive ORN inputs with similar concentration dependence and scaling patterns (Figs. 1 and 4). Second, most mPNs were electrically coupled with mPNs reciprocally, a situation facilitating synchronization of activities (Figs. 2 and 3). Third, mPNs are GABAergic, which are known to be inhibitory in adult flies, whereas mPNs are excitatory cholinergic neurons; thus, they are likely to have opposite actions on downstream neurons. Moreover, mPN axons are more likely to target downstream neurons of mPNs instead of mPN axons (Fig. 5), a situation favoring a postsynaptic inhibition model (43). These findings may provide insights into the structural and working principle of the olfactory

system in other insects, especially those that have multiglomerular GABAergic PNs (44, 45).

By performing multicolor calcium imaging, it is feasible to compare the physiological activities of different subsets of neurons evoked by the same stimuli, a useful method to study neural circuits systematically. For instance, our results showed that the odor-evoked response profiles of mPNs depend, to some degree, on their dendritic arborizations within the AL. The response profiles of mPN1s were similar to those of mPNs that innervated the same glomerulus, whereas mPN2s, which innervate multiple glomeruli, exhibited a relatively broader profile. These observations suggest that the response patterns of mPNs are largely determined by the inputs they receive from the AL. Further detailed knowledge of the intrinsic properties of each mPN subtype and their connectivities with other AL neurons (e.g., ORNs and inhibitory local interneurons) will facilitate the understanding of the structure–activity relationship of these neurons, as well as the physiological importance of such diverse odor-response profiles in conveying olfactory information.

In *Drosophila*, a global electrically coupled network, formed by the neurites of eLNs and mPNs, exists in ALs and is believed to mediate the excitatory crosstalk among different glomeruli (27, 30–32). However, the limited number of eLNs (two to three in each AL) and the low coupling efficacy between eLNs and mPNs appear to be insufficient to account for the strong lateral excitation found among glomeruli, suggesting that additional neuronal components may contribute to this network. Our functional studies demonstrated that the dendrites of most mPNs are electrically coupled with mPNs (Figs. 2 and 3), indicating that mPNs could fill this role. One important difference between eLNs and mPNs is that each eLN innervates most if not all glomeruli (32), whereas electrically coupled mPNs usually innervate single or a few glomeruli (18, 19). Therefore, whereas eLNs are responsible for global crosstalk, mPNs provide a means for communication among selected glomeruli. Indeed, selectivity was observed in interglomerular crosstalk triggered by either ORNs (27) or mPNs (Fig. 3). Thus, mPNs may complement the global effect of eLNs by enhancing the correlation of activities among selective glomeruli.

## Materials and Methods

**Fly Stocks.** All flies except those used in optogenetics experiments were reared on standard cornmeal–agar–molasses medium. The detailed genotypes of flies are listed in *SI Materials and Methods*.

**Generation of Transgenic Flies.** To create the *pUAST-R-GECO1* and *pQUAST-R-GECO1* constructs, the coding sequence of *R-GECO1* was amplified from the plasmid *CMV-R-GECO1* obtained from Addgene and subcloned into plasmids *pUAST* and *pQUAST*, respectively. Transgenic flies were generated by injecting the constructs into *w<sup>1118</sup>* embryos with a helper plasmid, crossing the injected flies with *w<sup>1118</sup>* flies, and selecting the positive offspring according to eye color. Transgenic lines with high expression levels and minimal leaky expression were chosen in this study. To increase the expression level of *R-GECO1*, alleles with two copies of *UAS-R-GECO1* inserted at different loci on the same chromosome were used.

**Electrophysiology.** To perform *ex vivo* recordings, flies ages 3–5 d were immobilized by cooling on ice for 15–30 s, and their brains were dissected out in extracellular solution. Recording was performed as described previously (24).

**Calcium Imaging.** Calcium imaging was performed at 20–22 °C under a Nikon-FN1 confocal microscope with a Nikon NIR Apo 40× water immersion objective (N.A. = 0.8) or a Nikon Apo LWD 25× water immersion objective (N.A. = 1.1). The responses were calculated using the Fiji image-analysis program and MATLAB software.

**Optogenetic Stimulation.** Flies used in optogenetic activation experiments were cultured on standard food plus 100 nM *all-trans*-retinal. A blue laser (473 nm) and a custom-built acousto-optic system (24) are used to selectively activate desired neurons.

More details are available in *SI Materials and Methods*.

**ACKNOWLEDGMENTS.** We thank Drs. Kristin Scott, Tzumin Lee, Kei Ito, Orie Shafer, Robert Wyman, Wang Jing, and Loren Looger for kindly sharing fly stocks; Drs. John Lin, Roger Y. Tsien, and Robert Campbell for generously providing plasmids; Dr. Christopher Potter for advice on using the Q-system; Dr. Aike Guo and the members of his laboratory for helpful suggestions on the experiment; Dr. Qian Hu and the Optical Imaging Facility for their

assistance in the imaging experiments; and especially Dr. Mu-ming Poo for critical reading of the manuscript. This work was supported by the "Strategic Priority Research Program (B)" of the Chinese Academy of Sciences (Grant XDB02010005) and China 973 Project (Grant 2011CBA0040) (to Z.W.) and the National Nature Science Foundation of China (Grants 30925013 and 81327802) (to S.Z.).

- Galizia CG, Rössler W (2010) Parallel olfactory systems in insects: Anatomy and function. *Annu Rev Entomol* 55:399–420.
- Martin JP, et al. (2011) The neurobiology of insect olfaction: Sensory processing in a comparative context. *Prog Neurobiol* 95(3):427–447.
- Stocker RF, Lienhard MC, Borst A, Fischbach KF (1990) Neuronal architecture of the antennal lobe in *Drosophila melanogaster*. *Cell Tissue Res* 262(1):9–34.
- Masse NY, Turner GC, Jefferis GS (2009) Olfactory information processing in *Drosophila*. *Curr Biol* 19(16):R700–R713.
- Vosshall LB, Stocker RF (2007) Molecular architecture of smell and taste in *Drosophila*. *Annu Rev Neurosci* 30:505–533.
- Wilson RI, Mainen ZF (2006) Early events in olfactory processing. *Annu Rev Neurosci* 29:163–201.
- Brill MF, et al. (2013) Parallel processing via a dual olfactory pathway in the honeybee. *J Neurosci* 33(6):2443–2456.
- Carcaud J, Hill T, Giurfa M, Sandoz JC (2012) Differential coding by two olfactory subsystems in the honeybee brain. *J Neurophysiol* 108(4):1106–1121.
- Galizia CG, Franke T, Menzel R, Sandoz JC (2012) Optical imaging of concealed brain activity using a gold mirror in honeybees. *J Insect Physiol* 58(5):743–749.
- Rössler W, Brill MF (2013) Parallel processing in the honeybee olfactory pathway: Structure, function, and evolution. *J Comp Physiol A Neuroethol Sens Neural Behav Physiol* 199(11):981–996.
- Schmucker M, Yamagata N, Nawrot MP, Menzel R (2011) Parallel representation of stimulus identity and intensity in a dual pathway model inspired by the olfactory system of the honeybee. *Front Neuroeng* 4:17.
- Riffell JA, Lei H, Abrell L, Hildebrand JG (2013) Neural basis of a pollinator's buffet: Olfactory specialization and learning in *Manduca sexta*. *Science* 339(6116):200–204.
- Silbering AF, Okada R, Ito K, Galizia CG (2008) Olfactory information processing in the *Drosophila* antennal lobe: Anything goes? *J Neurosci* 28(49):13075–13087.
- Wang JW, Wong AM, Flores J, Vosshall LB, Axel R (2003) Two-photon calcium imaging reveals an odor-evoked map of activity in the fly brain. *Cell* 112(2):271–282.
- Wilson RI, Turner GC, Laurent G (2004) Transformation of olfactory representations in the *Drosophila* antennal lobe. *Science* 303(5656):366–370.
- Heimbeck G, Bugnon V, Gendre N, Keller A, Stocker RF (2001) A central neural circuit for experience-independent olfactory and courtship behavior in *Drosophila melanogaster*. *Proc Natl Acad Sci USA* 98(26):15336–15341.
- Semmelhack JL, Wang JW (2009) Select *Drosophila* glomeruli mediate innate olfactory attraction and aversion. *Nature* 459(7244):218–223.
- Lai SL, Awasaki T, Ito K, Lee T (2008) Clonal analysis of *Drosophila* antennal lobe neurons: Diverse neuronal architectures in the lateral neuroblast lineage. *Development* 135(17):2883–2893.
- Tanaka NK, Endo K, Ito K (2012) Organization of antennal lobe-associated neurons in adult *Drosophila melanogaster* brain. *J Comp Neurol* 520(18):4067–4130.
- Ito K, Sass H, Urban J, Hofbauer A, Schneuwly S (1997) GAL4-responsive UAS-tau as a tool for studying the anatomy and development of the *Drosophila* central nervous system. *Cell Tissue Res* 290(1):1–10.
- Kazama H, Wilson RI (2008) Homeostatic matching and nonlinear amplification at identified central synapses. *Neuron* 58(3):401–413.
- Ng M, et al. (2002) Transmission of olfactory information between three populations of neurons in the antennal lobe of the fly. *Neuron* 36(3):463–474.
- Lin JY, Lin MZ, Steinbach P, Tsien RY (2009) Characterization of engineered channel-rhodopsin variants with improved properties and kinetics. *Biophys J* 96(5):1803–1814.
- Wang K, et al. (2011) Precise spatiotemporal control of optogenetic activation using an acousto-optic device. *PLoS ONE* 6(12):e28468.
- Potter CJ, Tasic B, Russler EV, Liang L, Luo L (2010) The Q system: A repressible binary system for transgene expression, lineage tracing, and mosaic analysis. *Cell* 141(3):536–548.
- Curtin KD, Zhang Z, Wyman RJ (2002) Gap junction proteins are not interchangeable in development of neural function in the *Drosophila* visual system. *J Cell Sci* 115(Pt 17):3379–3388.
- Olsen SR, Bhandawat V, Wilson RI (2007) Excitatory interactions between olfactory processing channels in the *Drosophila* antennal lobe. *Neuron* 54(1):89–103.
- Okada R, Awasaki T, Ito K (2009) Gamma-aminobutyric acid (GABA)-mediated neural connections in the *Drosophila* antennal lobe. *J Comp Neurol* 514(1):74–91.
- Shang Y, Claridge-Chang A, Sjulson L, Pypaert M, Miesenböck G (2007) Excitatory local circuits and their implications for olfactory processing in the fly antennal lobe. *Cell* 128(3):601–612.
- Huang J, Zhang W, Qiao W, Hu A, Wang Z (2010) Functional connectivity and selective odor responses of excitatory local interneurons in *Drosophila* antennal lobe. *Neuron* 67(6):1021–1033.
- Yakshi E, Wilson RI (2010) Electrical coupling between olfactory glomeruli. *Neuron* 67(6):1034–1047.
- Tootoonian S, Laurent G (2010) Electric times in olfaction. *Neuron* 67(6):903–905.
- Li H, Li Y, Lei Z, Wang K, Guo A (2013) Transformation of odor selectivity from projection neurons to single mushroom body neurons mapped with dual-color calcium imaging. *Proc Natl Acad Sci USA* 110(29):12084–12089.
- Tian L, et al. (2009) Imaging neural activity in worms, flies and mice with improved GCaMP calcium indicators. *Nat Methods* 6(12):875–881.
- Yao Z, Macara AM, Lelito KR, Minoyan TY, Shafer OT (2012) Analysis of functional neuronal connectivity in the *Drosophila* brain. *J Neurophysiol* 108(2):684–696.
- Zhao Y, et al. (2011) An expanded palette of genetically encoded Ca<sup>2+</sup> indicators. *Science* 333(6051):1888–1891.
- Jefferis GS, et al. (2007) Comprehensive maps of *Drosophila* higher olfactory centers: Spatially segregated fruit and pheromone representation. *Cell* 128(6):1187–1203.
- Tanaka NK, Awasaki T, Shimada T, Ito K (2004) Integration of chemosensory pathways in the *Drosophila* second-order olfactory centers. *Curr Biol* 14(6):449–457.
- de Belle JS, Heisenberg M (1994) Associative odor learning in *Drosophila* abolished by chemical ablation of mushroom bodies. *Science* 263(5147):692–695.
- Kido A, Ito K (2002) Mushroom bodies are not required for courtship behavior by normal and sexually mosaic *Drosophila*. *J Neurobiol* 52(4):302–311.
- Dietzl G, et al. (2007) A genome-wide transgenic RNAi library for conditional gene inactivation in *Drosophila*. *Nature* 448(7150):151–156.
- Liu X, Davis RL (2009) The GABAergic anterior paired lateral neuron suppresses and is suppressed by olfactory learning. *Nat Neurosci* 12(1):53–59.
- Liang L, et al. (2013) GABAergic projection neurons route selective olfactory inputs to specific higher-order neurons. *Neuron* 79(5):917–931.
- Bicker G, Kreissl S, Hofbauer A (1993) Monoclonal antibody labels olfactory and visual pathways in *Drosophila* and *Apis* brains. *J Comp Neurol* 335(3):413–424.
- Hoskins SG, Homberg U, Kingan TG, Christensen TA, Hildebrand JG (1986) Immunocytochemistry of GABA in the antennal lobes of the sphinx moth *Manduca sexta*. *Cell Tissue Res* 244(2):243–252.